VI ITALIAN CONFERENCE OF RESEARCHERS IN GEOTECHNICAL ENGINEERING –
Geotechnical Engineering in Multidisciplinary Research: from Microscale to Regional Scale,
CNRIG2016

1D seismic response analysis of soil-building systems including failure shear mechanisms

Giuseppe Tropeano[a,*], Lorenza Evangelista[b], Francesco Silvestri[c], Anna d'Onofrio[c]

[a]DICAAR, University of Cagliari, piazza d'Armi, Cagliari 09123, Italy
[b]IAMC–CNR, Institute for Coastal Marine Environment, Calata Porta di Massa, 80133 Napoli, Italy
[c]DICEA, University of Naples Federico II, via Claudio 21, Naples 80125, Italy

Abstract

Modelling of soil shear rupture due to an earthquake is not generally implemented in the common codes for 1D seismic response analysis. It requires the use of advanced plasticity-based constitutive models of soil, that are often neglected in practice. A good balance between simplicity and reliability can be achieved with methods based on simplified formulations of the mathematical equations and of the constitutive models. The paper presents a computer code based on this philosophy conceived, addressed and optimised to reliably model both the 'transient' seismic response ('stick' mode) and the permanent deformation mechanisms accounting for the coupled effects of deformability and strength ('slip' mode). The code can be adopted to evaluate the seismic performance of different geotechnical systems that can be reasonably approximated to a 1D problem. In the paper, the code is applied to model a soft-storey failure occurred in a framed structure heavily damaged during a strong-motion earthquake.
© 2016 The Authors. Published by Elsevier Ltd. This is an open access article under the CC BY-NC-ND license
(http://creativecommons.org/licenses/by-nc-nd/4.0/).
Peer-review under the responsibility of the organizing and scientific committees of CNRIG2016

Keywords: seismic response analysis; soil-building system; shear failure; stick-slip model

1. Introduction

The 1D seismic site response can be performed using different numerical methods for the solution of the ground motion equations, depending on the subsoil discretization approach (i.e. continuous layers vs. finite elements) and on the adopted cyclic soil-behaviour model (i.e. linear equivalent vs. non-linear methods) [1]. The most widespread

---

* Corresponding author. Tel.: +39-070-675-5526; fax: +39-070-675-5523
  E-mail address: giuseppe.tropeano@unica.it

computer codes describe partially dynamic soil behaviour and do not guarantee a reasonable solution of the ground motion equations when large strains and failure conditions are reached. These aspects can be modelled by advanced computer codes implementing plasticity-based constitutive models for the dynamic soil behaviour. In practice, these are not widespread, because these models often require cumbersome calibration through detailed laboratory cyclic tests and their effectiveness can be significantly reduced if they are not implemented with an appropriate numerical formulation. In addition, the achievement of failure conditions is a singularity of the system that cannot be evaluated with numerical methods which assume the continuity and the differentiability of the stress and strain variables.

A good-working compromise is adopting a simplified description of both the mathematical equations and of the constitutive soil model. To this aim, the procedure proposed by [2] based on stick-slip dynamics, was extended with more general assumptions and implemented in the SCOSSA (Seismic COde for Stick-Slip Analysis) code [3]. The paper summarizes the model formulation and describes its application to simulate the damage occurred in a framed structure during l'Aquila Earthquake in 2009.

2. The stick-slip model

The adopted dynamics of the stick-slip model refers to a lumped mass system, reproducing the seismic response of a vertical soil column either horizontally layered (Fig. 1) or sloped. Two stages of dynamic analysis can be identified: in the first ('stick') phase, the potentially unstable mass cumulates vibrational kinetic energy, that is converted into a frictional sliding mechanism during the second ('slip') stage.

In the stick phase, the seismic response in terms of absolute displacements, $\mathbf{u_a}$, to a base ground motion, $\ddot{u}_g$, can be computed by integrating the MDOF system equation:

$$\mathbf{M\ddot{u}_a + C\dot{u}_a + Ku_a = f} \tag{1}$$

where $\mathbf{M}$, $\mathbf{C}$ and $\mathbf{K}$ are the mass, damping and stiffness matrices, $\mathbf{f}$ is the vector of applied forces.

The forces, T, acting on a generic s layer are:

$$T = -m_T \ddot{u}_s - \mathbf{1^T M_s \ddot{u}} \tag{2}$$

where the first term is the inertial force induced by the absolute acceleration at the s-th layer, $\ddot{u}_s$, while the second results from the non-uniform relative acceleration profile, $\mathbf{\ddot{u}}$, within the sliding mass, referred to $\ddot{u}_s$.
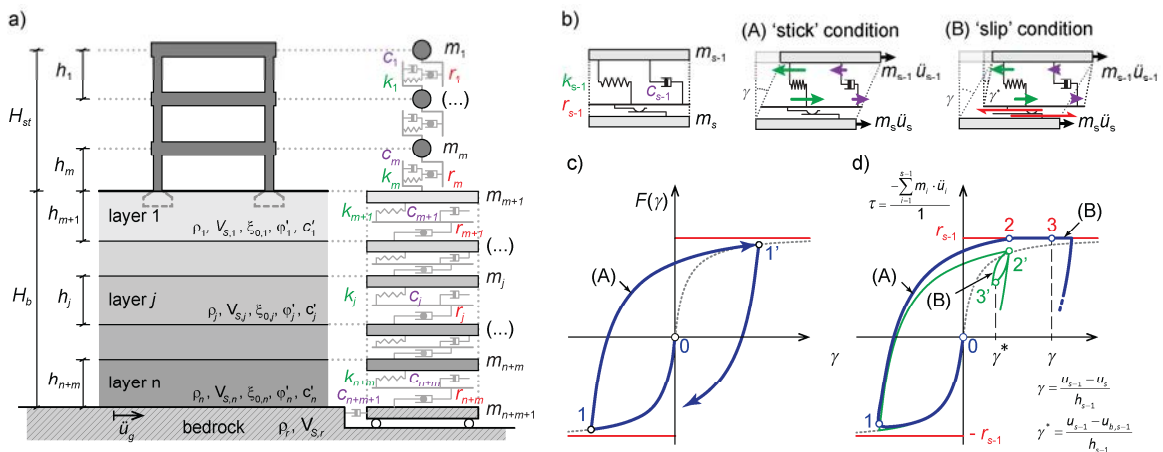

Fig. 1. (a) The MDOF system adopted in this study. (b) 'Stick' and 'slip' conditions in a two-mass system; (c) purely hysteretic behaviour; (d) dynamic response of the system.

The subscript '*S*' indicates sub-matrices and sub-vectors with index from 1 to (*s*-1); **1** is the unity vector.

At every time increment, the code checks if the inertial force, resulting from Eq. (2), is greater than or equal to the reaction of plastic slider, *r*, i.e. the resistance corresponding to the achievement of the limit shear force, $T_y = m_T \cdot a_y$, at each layer (where: m_T = total mass above the *s* layer base; a_y = yield acceleration). In such a case, the 'slip' conditions are triggered at the *s* layer base, and the equation of motion for the mass above this sliding surface (layer 1 to *s*-1) is given by the expression:

$$\mathbf{M_S}\ddot{\mathbf{u}} + \mathbf{C_S}\dot{\mathbf{u}} + \mathbf{K_S}\mathbf{u} = -\mathbf{M_S}\mathbf{1}\left(\ddot{u}_s + \ddot{u}_{b,s-1}\right) \tag{3}$$

while the response of the underlying (*n*-*s*+1) layers can be computed through a reduced system like that of Eq. (1). Along the sliding surface, the equilibrium during the slip is expressed by:

$$-m_T\left(\ddot{u}_s + \ddot{u}_{b,s-1}\right) - \mathbf{1}^T\mathbf{M_S}\ddot{\mathbf{u}} = -m_T a_y \tag{4}$$

Substituting Eq. (4) in Eq. (3), the equation for the 'slip' conditions is obtained as:

$$\left(\mathbf{M_S} - \frac{1}{m_T}\mathbf{M_S} \cdot \mathbf{1} \cdot \mathbf{1}^T\mathbf{M_S}\right)\ddot{\mathbf{u}} + \mathbf{C_S}\dot{\mathbf{u}} + \mathbf{K_S}\mathbf{u} = \mathbf{M_S}\mathbf{1} \cdot a_y \tag{5}$$

Solving Eq. (5) in terms of nodal relative acceleration, $\ddot{\mathbf{u}}$, the sliding acceleration time histories, $\ddot{u}_{b,s-1}$, at the base of the (*s*-1)[th] layer are obtained from Eq. (4). The relative sliding displacement, $u_{b,s-1}$, is computed by integrating twice the corresponding acceleration, as long as the sliding velocity, $\dot{u}_{b,s-1}$ is greater than 0. The above algorithm was implemented in the numerical code SCOSSA, in which the discretization of the subsoil profile into a lumped parameters system is optimized with reference to the soil shear wave velocity and the maximum input frequency [4].

The viscous damping matrix, **C**, is defined according to the full Rayleigh damping formulation [5] and the non-linear hysteretic response of the springs is modelled with an extended version of the modified hyperbolic model, MKZ [6], with original or modified Masing rules [7,8].

Figure 1b illustrates the performance of the constitutive model for the generic (*s*-1)[th] layer. The masses *s*-1 and *s* are connected by a non-linear hysteretic spring (k_{s-1}), a viscous dashpot (c_{s-1}) and a plastic slider (r_{s-1}). Under static load, the MKZ model uses two relationships: $F_{bb}(\gamma)$ for first loading (e.g. 0-1 in Fig. 1c) and $F_{ur}(\gamma)$ for unloading-reloading paths (e.g. 1-1' in Fig. 1c). The limiting strength is reached asymptotically when MKZ model degenerates to the hyperbolic stress-strain relationship. In dynamic 'stick' conditions (see pattern A and the corresponding point on the reloading curve in Fig. 1d), the current value of shear stress, τ, is computed considering the dynamic equilibrium of soil column (Eq. 1). As a consequence, the γ-τ relationship deviates from the purely hysteretic response (dashed line in Fig. 1d), shows rounded edges (point 1) and possibly reaches the limit strength (point 2) attaining the 'slip conditions' (pattern B in Fig. 1b). Thereafter, the shear stress holds constant until the system accumulates plastic straining, while the hysteretic response of the spring results into a small unloading-reloading cycle (Fig. 1d), induced by the application of modified Masing rules. Due to slippage, the subsystem above the sliding base is characterized by an actual value of the shear strain in a generic instant (indicated as γ^* in Fig. 1b,d) lower than the total strain, γ.

3. Application case

The above procedure was applied to model the seismic response of a soil-building system deeply investigated after the Abruzzo earthquake of April 6, 2009 ($M_w = 6.3$). Figure 2 shows the studied area, where seven similar r.c. buildings had suffered an uneven damage: two buildings collapsed suffering a soft-storey mechanism, while the remaining five showed only minor, non-structural damages. The area, located at the toe of Pettino mountain, is entirely settled on weathered and fine debris fan (Fig. 3), overlying a gravelly debris layer, that covers a finer alluvial silt on the top the calcareous bedrock.
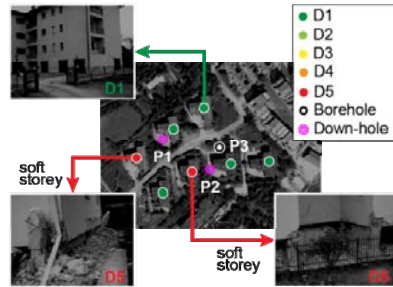
Fig. 2. Map of the studied area with the details of the non uniform damage [9].

Figure 3a shows the results of the P1 down-hole test executed near to the buildings (see Fig. 2).

The non-linear soil behavior was modeled through the variation of the normalized stiffness, G/G_0, and damping ratio, D, versus shear strain, γ (Fig. 3b), obtained experimentally through laboratory tests on similar soil sample taken in the Aterno valley [10].

The reference input motion was back-figured from the recorded mainshock at AQG station, located at the top of a moderately steep slope of weak partially fractured rock at about 1.5 km from Pettino site. Therefore, to estimate the reference bedrock motion, the ground motion recorded at AQG needed to be preliminarily reduced for a topographic amplification factor (1.2 was considered to be pertaining to the slope) and then projected along the directions normal (FN) and parallel (FP) to the fault that generated the event. Thereafter, both components were deconvoluted to the bedrock, considering the shear wave velocity profile obtained by a down-hole test carried out near the AQG station [11], obtaining the signals plotted in Figure 3c.

The formulation of SCOSSA permitted the dynamic analysis of the system consisting of the layered soil and the multi-storey building, modelling this latter as a continuous equivalent medium as well as the underlying soils. The structure was considered as a shear-type frame, with only the inertial masses of the rigid slabs and beams contributing to the actions on the columns. Information about the building foundations were not available; therefore, the mass and the stiffness of foundation structures were supposed as embedded in those of the first soil layer.

The analysed frame can be considered as representative of the average structural typology of the damaged buildings. It consists of three slabs, with inter-story of 3 m, and of 8 columns (0.3×0.5 m) with elastic modulus $E = 27000$ MPa [12]. The stiffness of the floors were obtained from the force-displacement diagrams ('capacity curves') of the pushover analysis (Fig. 4a).
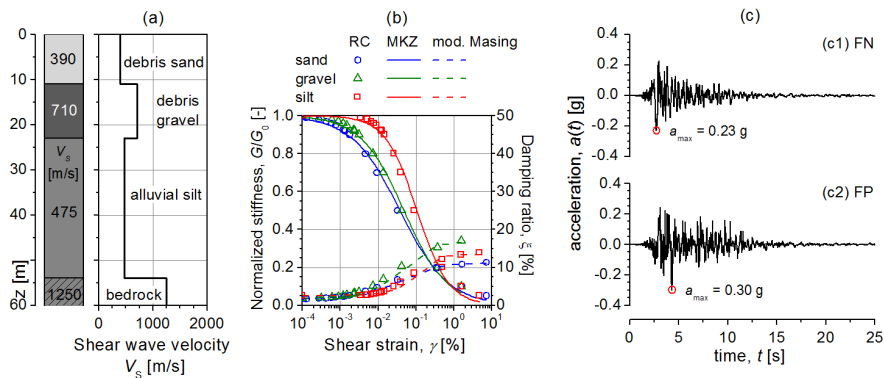

Fig. 3. (a) Layering and shear wave velocity profile obtained by a down-hole test in the Pettino area. (b) Non-linear properties of soils used in the numerical analyses and (c) acceleration time history of l'Aquila Earthquake recorded at AQG station, deconvoluted at bedrock and projected along the c1) fault normal (FN) and c2) fault parallel directions (FP).
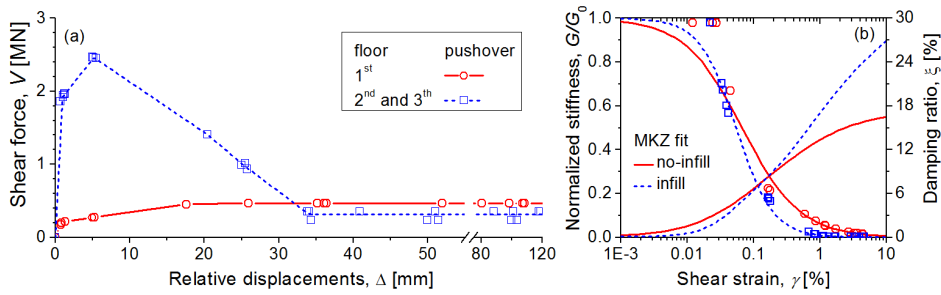
Fig. 4. (a) Push-over capacity curves, (b) fitting of stiffness reduction with modified hyperbolic model (MKZ) and hysteretic damping estimated using modified Masing criteria [11].

In particular, the initial stiffness, G_0, is the slope of the capacity curve at small displacements interpreted in terms of stress-strain relationship: namely, the storey force was divided by the frame footprint area ($A_t = 8.4$ m^2) and the shear strain was approximated with the ratio between the floors relative displacement and their inter-storey height. The first no-infill floor resulted characterized by an initial shear modulus, G_0, equal to 86 MPa, while that of the filled floors was equal to 985 MPa.

From the capacity curves, it was possible to evaluate the decay curve of the normalized stiffness as a function of shear strain, according to the modified hyperbolic model (MKZ) implemented in SCOSSA (Fig. 4b). The decay of stiffness obtained applying the MKZ fit to both pushover curves interpolates the points of the capacity curve quite satisfactorily at shear strains higher than 0.03%. The curve derived for the second and the third floors correctly describes the pre-peak behavior; however, the post-peak phase was not described with the same relationship, because the extended Masing criteria cannot reproduce a softening behavior, unless defining an adequate decay law of the initial stiffness. Therefore, the MKZ relationship can be considered as effective in the monotonically increasing part of the capacity curve, i.e. provided that the shear forces induced on the columns do not reach the peak values; such an assumption was then verified in the results of the numerical analyses. The hysteretic damping-strain curves estimated using the Masing criteria coherently describe a more pronounced dissipative behaviour for the infilled structure with respect to that without infill.

The contribution of viscous damping was neglected for the structure, while the achievement of shear failure conditions was modelled by introducing a plastic slider, for each soil layer and for each floor of the structure. The limit stress value was respectively derived from the soil strength parameters and from shear force corresponding to the maximum of the floor capacity curves. The results of the analyses are shown in Figure 5 in terms of peak acceleration profiles for both FN (a, b) and FP (c, d) components.

The analyses were performed considering free-field conditions (green dotted lines) and two structural patterns for the first structural level, i.e. with (blue dashed lines) or without (red solid lines) infill walls.
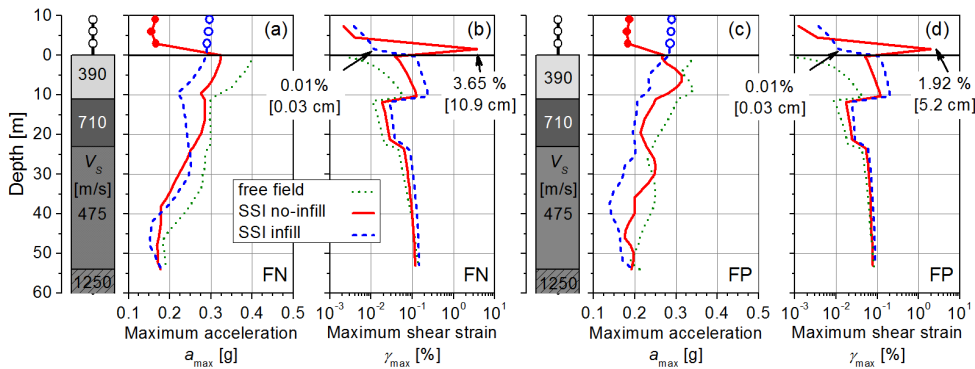

Fig. 5. Peak acceleration (a, c) and shear strain profiles (b, d) for different ground motion components and soil-structure patterns.

A significant reduction of the motion in the first soil layer with respect to the free field conditions is observed for both structural patterns, in particular with the FN input motion. The 'no-infill' pattern shows a considerable reduction of the peak acceleration at the slab levels, due to the high strain values reached at the first 'soft storey', as Figures. 5b-d show. More in detail, the maximum inter-storey strain was equal to approximately 3.65% and 1.92%, for the FN and FP components respectively, corresponding to a maximum displacement of the first slab approximately equal to 10.9 cm and 5.2 cm. In general, the reduction of the surface motion observed in both SSI analyses can be ascribed to the increase of soil strain, due to the high reduction of stiffness in the uppermost soil layer (for infill pattern) or of the first structural level (for no-infill pattern).

4. Conclusions

A lumped parameters model accounting for non-linear soil behaviour was implemented in the computer code SCOSSA, in order to assess the dynamic ground motion and the sliding displacements of a 1D soil layering, as well as aiming at including simplified structural models in the seismic response analyses. A soft-storey failure, occurred in a framed structure during the l'Aquila Earthquake, was modelled. In the analyses of the soil-structure system, it was considered a building with three floors, the first of which without infill. The results clearly showed the occurrence of a failure mechanism at the first structural level, with a strain increase capable to damp the motion and the inertial actions transmitted to the overlying floors. This mechanism is almost exclusively associated with the mechanical behavior of the elements of the first level. Despite the significant simplifications introduced in this simulation, the results seem compatible with the soft-storey mechanisms observed on the most damaged buildings.

To assess the role of infill walls, the same analyses were performed considering the fully filled frame. The structural stiffening induced an increase of the slab acceleration, and a significant reduction of the surface ground motion. The reduction of the surface motion observed in both SSI analyses can be ascribed to the increase of soil strain, due to the high reduction of stiffness at the first structural level (for no-infill pattern) or in the uppermost soil layer (for infill pattern). The strain level induced, however, were not high enough to induce any sliding mechanism in the soil.

Further developments for improving the reliability of the dynamic response of soil-structure systems might be the use of more refined structural capacity models and the introduction of suitable foundation model elements.

References

[1] J. Regnier et al., International benchmark on numerical simulations for 1D, non-linear site response (PRENOLIN): verification phase based on canonical cases, Bulletin of the Seismological Society of America, 2016 (submitted).

[2] E. Ausilio, A. Costanzo, F. Silvestri, G. Tropeano, Prediction of seismic slope displacements by dynamic stick-slip analyses, AIP Conference Proceedings. 1020 (2008) 475–484.

[3] G. Tropeano, A. Chiaradonna, A. d'Onofrio, F. Silvestri, An innovative computer code for 1D seismic response analysis including shear strength of soils, Geotechnique. 66 (2016) 95–105.

[4] J. Lysmer, R. Kuhlemeyer, Finite dynamic model for infinite media, Jour. of the Engineering Mechanics Division 95 (1969) 859–877.

[5] Y. Hashash, D. Park, Viscous damping formulation and high frequency motion propagation in non-linear site response analysis, Soil Dynamics and Earthquake Engineering. 22 (2002) 611–624.

[6] N. Matasovic, M. Vucetic, Generalized cyclic-degradation-pore pressure generation model for clays, Jour. of Geot. Eng . 121 (1995) 33–42.

[7] G. Masing, Eigenspannungen und verfestigung beim messing, Proceedings of the 2nd Int. Congress of Applied Mechanics. (1926) 332–335.

[8] C. Phillips, Y. Hashash, Damping formulation for nonlinear 1d site response analyses, Soil Dyn. and Earth. Eng.. 29 (2009) 1143–1158.

[9] G. Lanzo, G. Di Capua, R. Kayen, S. Kieffer, E. Button, G. Biscontin, G. Scasserra, P. Tommasi, A. Pagliaroli, F. Silvestri, A. d'Onofrio, C. Violante, A. Simonelli, R. Puglia, G. Mylonakis, G. Athanasopoulos, V. Vlahakis, J. Stewart, Seismological and geotechnical aspects of the M_w = 6.3 l'Aquila earthquake in central Italy on 6 April 2009. International Journal of Geoengineering case histories. 1 (2010), 206-339.

[10] A. d'Onofrio, L. Evangelista, L. Landolfi, F. Silvestri, D. Boiero, S. Foti, M. Maraschini, C. Comina, F. Santucci de Magistris. Geotechnical characterization of the C.A.S.E. project sites. Proc. Master MICA Innovazione nella Progettazione, Riabilitazione e Controllo delle Strutture: valutazione e Adeguamento in Zona Sismica, Università di Roma 3, 19-20 Aprile 2010, Roma, Italia.

[11] G. Tropeano, L. Evangelista, A. d'Onofrio, F. Silvestri, P. Ricci, G.M. Verderame, Il ruolo degli effetti di sito sulla risposta strutturale degli edifici nella conca aquilana, Proc of the 14[Th] Nat. Conf. on Earth. Eng..in Italy (ANIDIS 2011)", Bari, 18 – 22 settembre 2011. (in Italian).

[12] G.M.Verderame, F. De Luca, P. Ricci, G. Manfredi, Preliminary analysis of a soft-storey mechanism after the 2009 L'Aquila earthquake. Earthquake Engineering and Structural Dynamics. 40 (2011) 925–944.